Localization and segmentation of optic disc in retinal images using Circular Hough transform and Grow Cut algorithm (#8743)

First submission

Please read the **Important notes** below, and the **Review guidance** on the next page.
When ready **submit online**. The manuscript starts on page 3.

Important notes

Editor and deadline

Henkjan Huisman / 15 Feb 2016

Files	Please visit the overview page to **download and review** the files not included in this review pdf.
Declarations	No notable declarations are present

Review guidelines

Please in full read before you begin

How to review

When ready **submit your review online**. The review form is divided into 5 sections. Please consider these when composing your review:

1. **BASIC REPORTING**
2. **EXPERIMENTAL DESIGN**
3. **VALIDITY OF THE FINDINGS**
4. General comments
5. Confidential notes to the editor

You can also annotate this **pdf** and upload it as part of your review

To finish, enter your editorial recommendation (accept, revise or reject) and submit.

BASIC REPORTING

- Clear, unambiguous, professional English language used throughout.
- Intro & background to show context. Literature well referenced & relevant.
- Structure conforms to **PeerJ standard**, discipline norm, or improved for clarity.
- Figures are relevant, high quality, well labelled & described.
- Raw data supplied (See **PeerJ policy**).

EXPERIMENTAL DESIGN

- Original primary research within **Scope of the journal**.
- Research question well defined, relevant & meaningful. It is stated how research fills an identified knowledge gap.
- Rigorous investigation performed to a high technical & ethical standard.
- Methods described with sufficient detail & information to replicate.

VALIDITY OF THE FINDINGS

- Impact and novelty not assessed. Negative/inconclusive results accepted. *Meaningful* replication encouraged where rationale & benefit to literature is clearly stated.
- Data is robust, statistically sound, & controlled.
- Conclusion well stated, linked to original research question & limited to supporting results.
- Speculation is welcome, but should be identified as such.

The above is the editorial criteria summary. To view in full visit **https://peerj.com/about/editorial-criteria/**

Localization and segmentation of optic disc in retinal images using Circular Hough transform and Grow Cut algorithm

Muhammad Abdullah, Muhammad Moazam Fraz, Sarah Barman

Automated retinal image analysis has been emerging as an important diagnostic tool for early detection of eye related disease such as glaucoma and diabetic retinopathy. In this paper, we have presented a robust methodology for optic disc detection and boundary segmentation, which can be seen as the preliminary step in the development of a computer-assisted diagnostic system for glaucoma in retinal images. The proposed method is based on morphological operations, Circular Hough transform and Grow Cut algorithm. The morphological operators are used to enhance the optic disc and remove the retinal vasculature and other pathologies. The optic disc center is approximated using the Circular Hough Transform, and the Grow Cut algorithm is employed to precisely segment the optic disc boundary. The method is quantitatively evaluated on five publicly available retinal image databases DRIVE, DIARETDB1, CHASE_DB1, DRIONS-DB, Messidor and one local Shifa Hospital Database. The method achieves optic disc detection success rate as 100% for these databases with the exception of 99.09% and 99.25% for the DRIONS-DB and Messidor databases respectively. The optic disc boundary detection achieved an average spatial overlap of 78.6%, 85.12%, 83.23%, 85.1%, 87.93% and 80.1% respectively for these databases. This unique method has shown significant improvement over existing methods in terms of detection and boundary extraction of the optic disc.

Localization and Segmentation of Optic Disc in Retinal Images using Circular Hough Transform and Grow Cut Algorithm

Muhammad Abdullah[1], Muhammad Moazam Fraz[2] and Sarah A. Barman[3]

[1] *School of Electrical Engineering and Computer Science, National University of Sciences and Technology, Sector H-12, Islamabad, 44000, Pakistan.*

[2] *Faculty of Science Engineering and Computing, Kingston University London, United Kingdom*

Corresponding Author:
Muhammad Moazam Fraz
Street Address:
School of Electrical Engineering and Computer Science, National University of Sciences and Technology, Sector H-12, Islamabad, 44000, Pakistan.

Email Address:
moazam.fraz@seecs.edu.pk

Phone:
00 92 51 9085 2179

Abstract

Automated retinal image analysis has been emerging as an important diagnostic tool for early detection of eye related disease such as glaucoma and diabetic retinopathy. In this paper, we have presented a robust methodology for optic disc detection and boundary segmentation, which can be seen as the preliminary step in the development of a computer-assisted diagnostic system for glaucoma in retinal images. The proposed method is based on morphological operations, Circular Hough transform and Grow Cut algorithm. The morphological operators are used to enhance the optic disc and remove the retinal vasculature and other pathologies. The optic disc center is approximated using the Circular Hough Transform, and the Grow Cut algorithm is employed to precisely segment the optic disc boundary. The method is quantitatively evaluated on five publicly available retinal image databases DRIVE, DIARETDB1, CHASE_DB1, DRIONS-DB, Messidor and one local Shifa Hospital Database. The method achieves optic disc detection success rate as 100% for these databases with the exception of 99.09% and 99.25% for the DRIONS-DB and Messidor databases respectively. The optic disc boundary detection achieved an average spatial overlap of 78.6%, 85.12%, 83.23%, 85.1%, 87.93% and 80.1% respectively for these databases. This unique method has shown significant improvement over existing methods in terms of detection and boundary extraction of the optic disc.

Keywords

Glaucoma Detection, Growcut Algorithm, Image Analysis, Optic Disc, Retinal Image Analysis

1. Introduction

Digital retinal images are widely used for early detection of retinal, ophthalmic and systemic diseases because they provide a non-invasive window to the human circularity system and associated pathologies (Jack J. Kanski & Brad Bowling 2015). Glaucoma and Diabetic Retinopathy (DR) are among major retinal disease which are the leading cause of vision loss and blindness in the working population (Federation 2013). Early detection of these disease by screening programs and subsequent treatment can prevent blindness. Computer aided diagnostic retinal image analysis is the first step in automated screening of these diseases in large population based studies (Fraz et al. 2015). The change in anatomical structures in human retina, which includes retinal vasculature, Optic Disc (OD), optic cup and retinal pathologies are the early diagnostic indicators of several diseases such as DR, Macula Edema and Glaucoma (Jack J. Kanski & Brad Bowling 2015). Among these, the OD is the most important feature because its visual aspects are central for glaucoma detection and other lesions assessment related to DR. The important anatomical structures presented in the retinal image are shown in Figure 1. OD detection is preliminary step for glaucoma screening, which is globally the second leading cause of blindness. Moreover, it helps in the detection and localization of other retinal structures which includes the fovea, macula and estimating vascular changes (Basit & Fraz 2015).

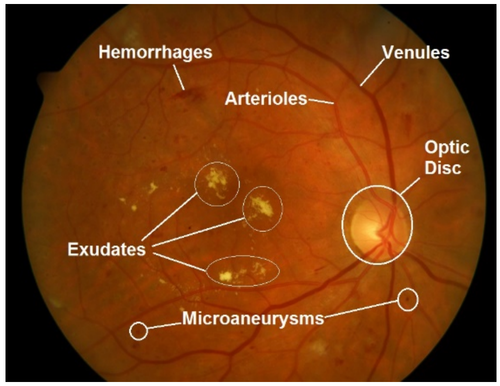

Figure 1 Important features in retinal fundus image.

Glaucoma is caused by the increase in the intraocular fluid pressure in the Optic Nerve Head (ONH), because of either blockage or a higher production of aqueous humor of the eye (Jack J. Kanski & Brad Bowling 2015). Glaucoma remains asymptomatic at an early stage and slowly progress with time which ultimately leads to blindness. Medical treatment is only effective at the early stages because the optic nerve, once damaged can't be cured (Weinreb et al. 2014). The early prevalence of Glaucoma can be identified by localization and segmentation of the OD and Optic Cup, followed by computing the cup-to-disc ratio. The structural changes in OD furnish critical clues pertaining to glaucoma prognosis (Abramoff et al. 2010). A Computer Assisted Diagnosis (CAD) system is necessary for large population based screening of Glaucoma. OD localization and segmentation is the first step towards the development of CAD. Knowing the significance such systems, several OD approaches have been proposed and attempted by many but it's still an active research area.

The OD appears as a variable sized, bright yellowish region, slightly oval in shape with blood vessels converging towards its center. These features are mostly used for automated OD localization. Retinal pathologies like exudates and lesions, if present, may appear like the shape of a disc, thus may cause false detection (Basit & Fraz 2015). In CAD, accurate detection and segmentation of the OD is quite a challenging task because of various factors like boundary artifacts, missing edges and poor textural contrast. The variation in illumination conditions, luminosity and contrast during image acquisition are added challenges (Haleem et al. 2013). Moreover, the OD boundary is not constant because of the presence of incoming blood vessels which produce a fused boundary. Another distractor is papillary atrophy which, if present, appears as the bright region outside the OD and thus deforms the OD boundary (Aquino et al. 2010).

This paper presents a new approach for automatic detection and segmentation of the OD based on morphological operations, Circular Hough Transform (CHT) (Illingworth & Kittler 1987) and Grow Cut (GC) algorithm (Vezhnevets & Konouchine 2005). The GC algorithm has been widely used in many application areas of image segmentation, but has not been applied within the framework of retinal image analysis. To the limit of our knowledge, the GC algorithm has been utilized for the first time in localizing and segmenting the OD in retinal images. The method is evaluated on five retinal image datasets exhibiting different morphological characteristics. Experimental evaluation shows that this method is computationally fast in processing, robust to the variation in image contrast and illumination, and comparable with the state-of-the-art methodologies in terms of quantitative performance metrics.

It's worth mentioning that this work is aimed at contributing to the development of automatic systems for glaucoma detection that are currently under development. Although other published

solutions can be used, this work presents higher accuracy, robustness and is tolerant to a vast variety of image characteristics, which make it suitable for integration with a glaucoma detection system.
The organization of the paper is as follows. Section 2 presents a comprehensive overview of the OD localization and segmentation methodologies available in the literature. Section 3 explains the proposed methodology in detail. The materials and the performance metrics used to evaluate the proposed methodology are illustrated in section 4. The results and comparison with other methods are given in section 5. The paper is concluded in section 6.

1 Related Work

A significant number of papers have been published to deal with the OD detection and segmentation (Haleem et al. 2013). Some papers only perform OD detection while others perform both detection and segmentation. Here we briefly discuss both of the groups.

1.1 Methods for OD detection

Hoover and Goldbaum (Hoover & Goldbaum 2003) use vascular origin to detect the OD center. To detect the vascular convergence point they use a fuzzy convergence and voting type algorithm. Niemeijer et al. (Niemeijer et al. 2009) performed vascular segmentation and measure the distance at specific locations with the help of a kNN regressor. The point with lowest distance to the OD is selected as the OD center. Inspired by results from vascular direction methods, Youssif et al. (Youssif et al. 2008) used a matched filter to match the direction of blood vessels around the OD area and a vessel direction map is obtained by segmenting vessels. Mendonca et al.(Mendonca et al. 2013) further improve the results by using the entropy of vascular direction to assess the convergence point of vessels. To increase robustness, they constrain the search for maximal entropy to the areas with high intensities. In (Lu 2011), a circular transformation is used to capture a circular shape OD and evaluate image variation along multiple radial lines. Pixels with maximum variations are determined, as they can be further used for OD center and boundary localization. Another methodology based on the Radon transformation of overlapping window (Pourreza-Shahri et al. 2014) has achieved 100% success in DRIVE and 96.3% on STARE databases.

1.2 Methods for OD detection and boundary segmentation

In (Welfer et al. 2010), a method based on mathematical morphology is proposed to detect and segment the OD in images from DRIVE and DIARETDB1. This work is extended in (Welfer et al. 2013) by incorporating a multiscale morphologic approach. Marin et al. (Marin et al. 2015) proposed a two step automatic thresholding on a morphologically processed bright enhanced region to get a reduced region of interest, followed by the application of Circular Hough Transformation (CHT) to get the OD center and OD region. Seo et al. (Seo et al. 2004) also use morphological and Canny edge detection filters to segment and detect the OD rim.
Kande et al. (Kande et al. 2008) detected the OD by using maximum local variance with 92.53% success rate and geometric Active Contour Model (ACM) for OD segmentation. In (Aquino et al. 2010), a template based approach is used for OD segmentation. They applied morphological and edge detection techniques followed by CHT to approximate circular objects. Lupascu et al. (Lupascu et al. 2008) used a regression method and texture descriptors for circular OD fitting. An approach based on Principal Component Analysis and mathematical modelling is presented in (Morales et al. 2013), which utilizes a generalized distance function, stochastic watershed and geodesic transformations. The result is finally approximated by a circular approximation. Walter et al. (Walter et al. 2002) presents a methodology based on Watershed transformation and

morphological processing. In (Hsiao et al. 2012), illumination correction technique was used to detect optic disc. They select high intensity pixels as candidates for OD and among those candidate pixels they select OD pixel as one with the highest variance. For segmentation, the Supervised Gradient Vector Flow (SGVF) snake model is used. By extending the SGVF snake in each iteration, contour points get updated and classified based on features. Statistical information and features extracted from trained images were then used for classification. In (Joshi et al. 2011), the Chan-Vese model has been extended by introducing image information around a contour point. Inspired by the work proposed in (Joshi et al. 2011), the local binary fitting energy ACM (Mittapalli & Kande 2016) is proposed to integrate the local image information which includes texture color and intensity for each point of interest. A multi-resolution Sliding Band Filter (SBF) was used in (Dashtbozorg et al. 2015) for OD segmentation. Super-pixels are employed in (Cheng et al. 2013) such that each super-pixel is classified as OD or non-OD. It has been observed that the confluence of vessels in the OD region affects the precision of OD segmentation methods. However, to overcome the influence of the presence of vessels some methods try to eliminate them from image. In this paper, we propose a new approach for automatic OD detection and segmentation which is not influenced by the confluence of vessels in OD area, therefore, no template or vessel map is required in advance.

2 The Methodology

This work presents an OD detection and segmentation methodology which is able to detect the OD center without using any template or prior vascular information. The OD appears as a yellowish structure in retinal fundus images with shape varying from circular to slightly elliptical and has the highest intensity value pixels. However, the presence of brightness artifacts can make the OD merge into the background and lose its brightness. Furthermore, the presence of several pathological structures such as exudates may take the shape of the OD and may have the highest intensity value. The proposed algorithm is based on morphological operations, Circular Hough transform and Grow Cut algorithm. The morphological operators are used to enhance the optic disc and remove the retinal vasculature and other pathologies. The optic disc center is approximated using the Circular Hough Transform, and the Grow Cut algorithm is employed to precisely segment the optic disc boundary.

2.1 Preprocessing

The variation in image contrast, background illumination and pigmentation is normalized by applying pre-processing operations to the retinal images.

The green channel of an RGB image gives maximum contrast between exudates and the neighboring regions (Fraz et al. 2012b). Therefore, the green channel of RGB images is processed for normalization of contrast and luminosity. A variety of algorithms for contrast and luminosity normalization in retinal images are available in the literature, and these methodologies are either based on subtracting the estimated background from the original image (Fraz et al. 2014) or on dividing the later by the former (Foracchia et al. 2005; Vázquez et al. 2013). However, experiments (Fraz et al. 2014) show that the results of both methods are similar with no appreciable advantage of one over the other. We have used the subtractive method as it has been reported in (Fraz et al. 2014). The background pixel intensities are estimated and the difference between the estimated background and the green channel is computed to produce the normalized image. The background of the retinal image, denoted as “Ibg” is estimated by applying a filtering operation with an arithmetic mean kernel. The size of the filter kernel is not a critical parameter as long as it is large enough to ensure the blurred image contains no visible structures such as optic disc, exudates or blood vessels. In this work, we have used an 89 × 89 pixel kernel. The difference between the estimated background "Ibg" and the morphologically opened image "Iopen" is calculated on pixel basis. Thus the background normalized image "Inorm" is obtained using:

$$I_{norm}(x, y) = I_{open}(x, y) - I_{bg}(x, y) \qquad (1)$$

Due to different illumination conditions in the acquisition process, there may be significant intensity variations between images. These intensity variations make it difficult to use the best possible technique for all of the images, thus shade corrections were necessary and have been applied. A global linear transformation function is applied to modify the pixel intensities.

$$I_{SC}(x, y) = \begin{cases} 0, & \text{if } I_{norm}(x, y) < 0 \\ 1, & \text{if } I_{norm}(x, y) < 0 \\ I_{adjusted}(x, y) & \text{otherwise} \end{cases} \qquad (2)$$

$$I_{adjusted}(x, y) = I_{norm}(x, y) - IntVal_{MaxPixels} + 0.5 \qquad (3)$$

Where $Isc\,(x,y)$ is the shade corrected image, $I_{norm}(x,y)$ is the background normalized image, $IntVal_{MostPixels}$ is the intensity value representing the most number of pixels in the normalized image $I_{norm}(x,y)$. Pixels with this intensity value $IntVal_{MostPixels}$ represent the background (Fraz et al. 2012a). This global transformation function normalizes or shade corrects the image by setting the background pixels to 0.5, which can be observed in Figure 2(c).

2.2 Optic Disc Detection

After pre-processing, the OD appears as the brightest structure in the image with varying size and appearance. The retinal blood vessels originate from the OD and branch out to spread in the retinal image. A morphological closing operation with a disc shaped structuring element is applied to the pre-processed image in order to remove the vasculature from the image. The result is shown in Figure 2(d).

CHT, an extension of Hough transform (HT) (Hough 1962), is for the detection of circular objects from the image. For the detection of a circle, the HT is based on the equation of circle, defined as

$$(x_i - a)^2 + (y_i - b)^2 = r^2 \qquad (4)$$

Where, "(a, b)" represents the coordinates of the center of the circle and "r" denotes the radius. In order to increase the robustness of CHT we resize all images to a common resolution and search for the bright circles with an experimented selected radius range of 29 to 50 pixels. To avoid false detection of OD we optimized our system by applying CHT on each image at different sensitivity levels and among circular responses generated by CHT we take only strong circle. Strong circles are the ones that correspond to the OD while the rest are either exudates or misleading regions. The results of intermediary processing steps for OD localization/detection are shown in Figure 2.

2.3 Optic Disc Segmentation

In the preprocessed image, the OD area is treated as foreground (fg) and the rest of the retinal image is considered as background (bg). The Grow Cut (GC) (Vezhnevets & Konouchine 2005) algorithm separates the fg from bg using the von Neumann Neighborhood principle (Toffoli & Margolus 1987) and seeded region growing. The detected OD center is chosen as initial seed points for fg area whereas the bg seed points are automatically chosen from rest of image. This algorithm iteratively checks each neighboring pixel and decides its region-wise membership. The GC algorithm use cellular automata for image modelling. Each image pixel "p" can be represented by a triplet (lp, θp, Cp). Where, lp represents the class label of the pixel, θp represents the "strength" of the pixel label assignment. I is a measure of the certainty of the pixel label. The label of a pixel whose "strength" = 1 cannot be changed during the algorithm progress, whereas the pixel label whose "strength" < 1 may change during algorithm execution. Cp represents the pixel greyscale value.

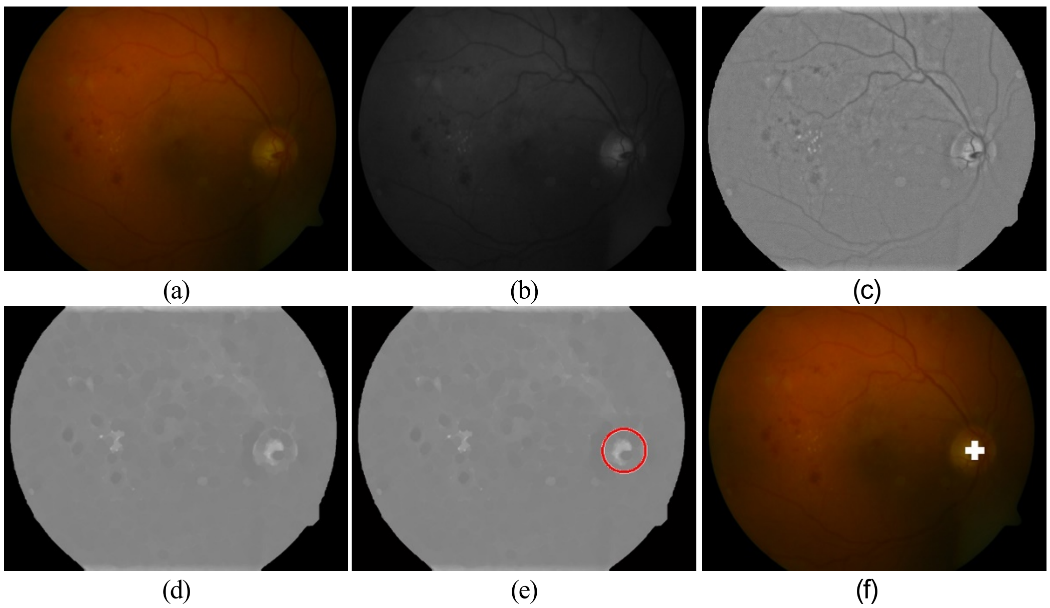

Figure 2 Processing steps for OD detection.

(a) RGB retinal image (b) Green Channel image (c) Preprocessed green channel image (d) Blood vessel removed image (e) Circular approximation of optic disc by CHT (f) Detected OD center

At the initial stage of the algorithm, the triplet for all pixels are set as,

$$l_p = 0,\ \theta_p = 0,\ C_p = RGB_p \qquad (5)$$

Which means that initially all pixels have undefined labels and zero strength. The aim of the GC algorithm in segmenting the OD is to assign a label to each pixel in the image regarding whether it belongs to OD or to the retinal image background. To start the algorithm, we initialized seeds by setting labels for the optic disc (+1) and non-OD (-1). Once the seeds are initialized, the process keeps on iteratively assigning labels to each pixel in the image until all pixels are labelled. For each pixel p and its neighbors xi (i=1 to 8), quantity "g" is computed which is monotonous decreasing function where g (xi) ∈ [0, 1] such that

$$g(x_i) = \frac{\| C_p - C_{xi} \|_2}{max \| C \|_2} \qquad (6)$$

As we were using green channel of the image so $\| C_p - C_{xi} \|$ is equal to $\| I_p - I_{x_i} \|$, where I_p and I_{x_i} are the intensities of pixels p and xi respectively. $max \| C \|_2$ is equal to 2L -1, where L is the bit depth of the image. Afterwards, the algorithm iteratively compute λ (xi) for all pixels xi which don't have label "undefined" such that:

$$\lambda(x_i) = g(x_i).\theta(x_i) \qquad (7)$$

If $\lambda(x_i) > \theta_p$ then a pixel takes the label and strength of xi otherwise it keeps its own label and "strength". The algorithm terminates when all the pixels are labeled and the pixel label stops changing. In the end, the segmented OD boundary is approximated to a circular shape. The processing steps of OD boundary extraction are shown in Figure 3. The circular approximation of the OD boundary is illustrated in Figure 4.

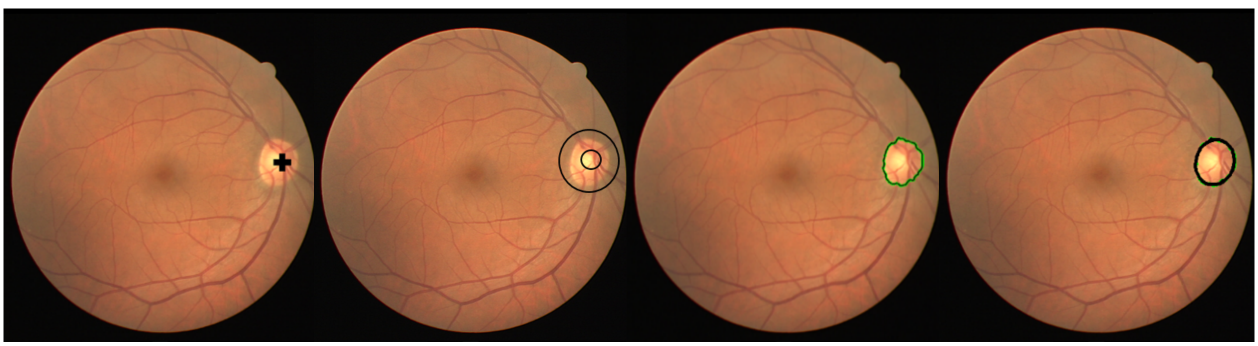

(a) (b) (c) (d)

Figure 3 Steps for OD boundary extraction

(A) Original RGB image with detected central point of optic disc, (B) Foreground (optic disc area represented by small circle) selection points and background (non-optic disc region represented by large circle) selection points (C) Result of Grow Cut for boundary segmentation, (D) Boundary approximation (in black) of grow cut.

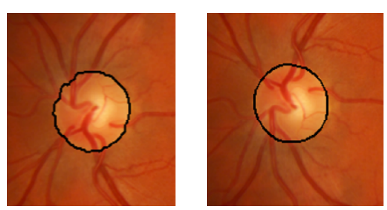

Figure 4 Close up view of (A) Grow Cut segmentation; (B) approximation of Grow Cut.

3 Materials

The proposed methodology is evaluated on five publicly available retinal image databases and one local database.

3.1 DRIVE

DRIVE (2004) is a publically available database consisting of 40 images with resolution 584 × 565 pixels. Out of these 40 images, 7 are pathological, containing pigment epithelium changes, exudates and hemorrhages.

3.2 DIARETDB1

The DIARETDB1 (Kauppi et al. 2007) database comprised 89 fundus images which are obtained with a 50° of FOV using a fundus camera and are in PNG format. These images are of size 1500 × 1152 pixels, with 24bits/pixel.

3.3 CHASEDB1

The CHASEDB1 (Fraz et al. 2012c) database consists of 28 images captured from a Nidek NM 200D camera at 30° FOV. Images are of 1280 × 960 pixels resolution, which are affected by illumination artifacts and poor contrast.

3.4 DRIONS-DB

The DRIONS (Carmona et al. 2008) database consists of 110 images of 600 ×400 resolution, with 8 bits/pixel. In these 110 images, 50 images contain some sort of defect, such as illumination artifacts, rim blurredness and papillary atrophy, which may hinder the detection and segmentation problem.

3.5 Messidor

The Messidor (Decenciere et al. 2014) database consists of 1200 retinal fundus images which were captured from 3CCD color video camera on Topcon TRC NW6 non-mydriatic retinograph, with 45° of FOV.

3.6 Shifa Database

This database belongs to Department of Ophthalmology, Shifa International Hospital Islamabad, Pakistan. 19 images are healthy while the rest of them have some sort pathological symptoms and illumination artifacts. The dataset consists of 111 fundus images of 1936 × 1296 resolution, acquired with a 45° field of view.

3.7 Ground Truths

The OD in all the images from the above mentioned databases is hand labelled by ophthalmic experts from the Armed Forces Institute of Ophthalmology, Rawalpindi, Pakistan and used as ground truths. For 1200 images in the Messidor database, we have used the ground truths provided by Aquino et.al (Aquino et al. 2010). The quantitative results are based on comparison of automatic segmented images with these ground truths.

3.8 Quantitative Performance Measures

The outcome of OD detection and the segmentation process results in the classification of pixels belong to OD region or non-OD region. There are four possibilities for pixel classification, illustrated in Table 1, True Positive (TP), True Negative (TN), False Positive (FP) and false Negative (FN). The first two are the result of mutual agreement between predicted values and actual values while the last two are the result of the wrong prediction. TP is the case when the system predicts the pixel belongs to the OD and is actually an OD pixel in reference to the ground truth image, while in the case of TN both the system and actual ground truth identify a pixel as a non-OD pixel. FP is the case where the system predicts the pixel as an OD pixel when it actually belongs to non-OD region in ground truth, whereas, in the FN case the system predicts a pixel as a non-OD pixel when it actually is an OD pixel.

The metrics used to evaluate the quantitative performance of the proposed methodology are given in Table 2. We used Sensitivity (SN), Specificity (SP), Accuracy (Acc), Positive Predicted Value (PPV), False Discovery Rate (FDR) and Overlap. The overlap metric is defined in (8).

$$\text{Overlap} = \frac{Area(ground\ truth \cap predicted)}{Area(ground\ truth \cup predicted)} \tag{8}$$

Moreover, we have used the DICE similarity index to measure the similarity between the segmented optic disc and the ground truth. The DICE index is a measurement of spatial overlap used widely for comparing segmentation results, with a value ranging from 0 to 1. The DICE coefficient can be defined as two times the volume of the intersection between two segmentations divided by the sum of the volumes of the two segmentations, which is represented in (9).

$$\text{DICE} = \frac{2 * Area\left(ground\ \ truth \cap \ \ predicted\right)}{Area(ground\ \ truth) + Area(\ predicted)} \qquad (9)$$

Table 1

Pixel classification

Real → Predicted ↓	Actual pixel ∈ OD	Actual pixel ∉ OD
System Predicted pixel ∈ OD	TP	FP
System Predicted pixel ∉ OD	FN	TN

Table 2

Performance metric for OD Segmentation

Measure	Description
SN	TP/(TP+FN)
SP	TN/(TN+FP)
Acc	(TP+TN)/(TP+FP+TN+FN)
PPV	TP/(TP+FP)
FDR	FP / (FP+TP)

4 Results

The optic disc detection method achieved 100% success rate in DRIVE, DIARETDB1, CHASE_DB1 and Shifa databases, it achieved 99.09% in DRIONS-DB and 99.25% in the Messidor database.

Table 3

Performance measures of OD segmentation

Performance Measure	DRIVE	DIARET DB1	CHASE-DB1	Shifa	DRIONS -DB	Messidor
Acc	0.9672	0.9772	0.9579	0.9793	0.9549	0.9989
SP	0.9966	0.9984	0.9971	0.9991	0.9966	0.9995
SN	0.8187	0.8510	0.8313	0.8015	0.8508	0.8954
PPV	0.8728	0.9263	0.9261	0.9493	0.9966	0.9794
FDR	0.1271	0.0737	0.0738	0.0506	0.0810	0.020
DICE	0.8720	0.8910	0.9050	0.8763	0.9102	0.9339
Overlap	78.6%	85.1%	83.2%	80.1%	85.1%	87.93%

The pixel-wise quantitative performance metrics (which are defined in Table 2) are calculated for OD segmentation, based on the comparison of automatic segmented images with the ground truth reference images and are illustrated in Table 3. The methodology is quantitatively evaluated by using an array of performance metrics, which to the limit of our knowledge has not been previously used for evaluating OD segmentation algorithms.

Table 4
Comparison with other methods

Performance Measures → Methods↓	Sensitivity	Specificity	Accuracy	DICE Score	Overlap %	Predictive Value	Time per image (in sec)
DRIVE Database							
Sopharak et al.(Sopharak et al. 2008)	0.2104	0.9993	--	--	16.88	0.9334	14.92
Walter et al. (Walter et al. 2002)	0.4988	0.9981	--	--	29.32	0.8653	219.6
Seo et al. (Seo et al. 2004)	0.5029	0.9983	--	--	31.09	0.843	7.23
Kande et al. (Kande et al. 2008)	0.6999	0.9888	--	--	29.66	0.5218	111.7
Sta, por et al.(Stapor et al. 2004)	0.7368	0.9920	--	--	33.42	0.6198	43.00
Lupascu et al (Lupascu et al. 2008)	0.7768	0.9968	--	--	30.95	0.88.14	--
D.Welfer et al. (Welfer et al. 2013)	0.7357	0.9982	--	--	39.40	0.8876	53.65
Basit et. al (Basit & Fraz 2015)	0.8921	0.9921	--	--	61.88	0.6930	--
Morales et. al(Morales et al. 2013)	--	--	0.9903	0.8169	--	0.8544	--
Salazar-Gonzalez et. al (Salazar-Gonzalez et al. 2014)	0.7512	0.9684	0.9412	--	--	--	--
Proposed Method	0.8188	0.9966	0.9672	0.8720	78.6	0.8728	59.2
DIARETDB1 Database							
Sopharak et al.(Sopharak et al. 2008)	0.4603	0.9994	--	--	29.41	0.9593	74.55
Walter et al. (Walter et al. 2002)	0.6569	0.9993	--	--	36.97	0.9395	308.5
Seo et al. (Seo et al. 2004)	0.6103	0.9987	--	--	35.32	0.8878	15.63
Kande et al. (Kande et al. 2008)	0.8808	0.9878	--	--	33.41	0.5448	120.5
Sta, por et al.(Stapor et al. 2004)	0.8498	0.9964	--	--	34.08	0.8034	59.72
Lupascu et al (Lupascu et al. 2008)	0.6848	0.9969	--	--	30.95	0.8117	--
D.Welfer et al. (Welfer et al. 2013)	0.6341	0.9981	--	--	39.15	0.8704	57.16
Basit et .al (Basit & Fraz 2015)	0.7347	0.9944	--	--	54.69	0.7049	--
Morales et. al (Morales et al. 2013)	--	--	0.9957	0.893	--	0.9224	--
Proposed Method	0.851	0.9984	0.9772	0.891	85.1	0.9263	40.0

The comparison of the proposed method has been made with other available methods on the basis of average sensitivity, specificity, accuracy, DICE score, overlap, positive predictive value and the time taken to process a single image, as illustrated in Table 4. Results shows that the proposed method provides promising results as compared to other OD segmentation techniques in the literature. The comparison with other methods is made with respect to DRIVE and DIARETDB1 because most of the available methods presents their results on these two databases.

Figure 5 shows the results of the OD detection in the DRIVE, DIARETDB1, Shifa, CHASE_DB1 and DRIONS-DB databases. The OD segmentation results on these retinal datasets are illustrated in Figure 6. It can be observed that the proposed methodology can successfully detect and segment the OD in the pathological images as well as in images with non-uniform illumination and uneven background pigmentation from multiple retinal image datasets.

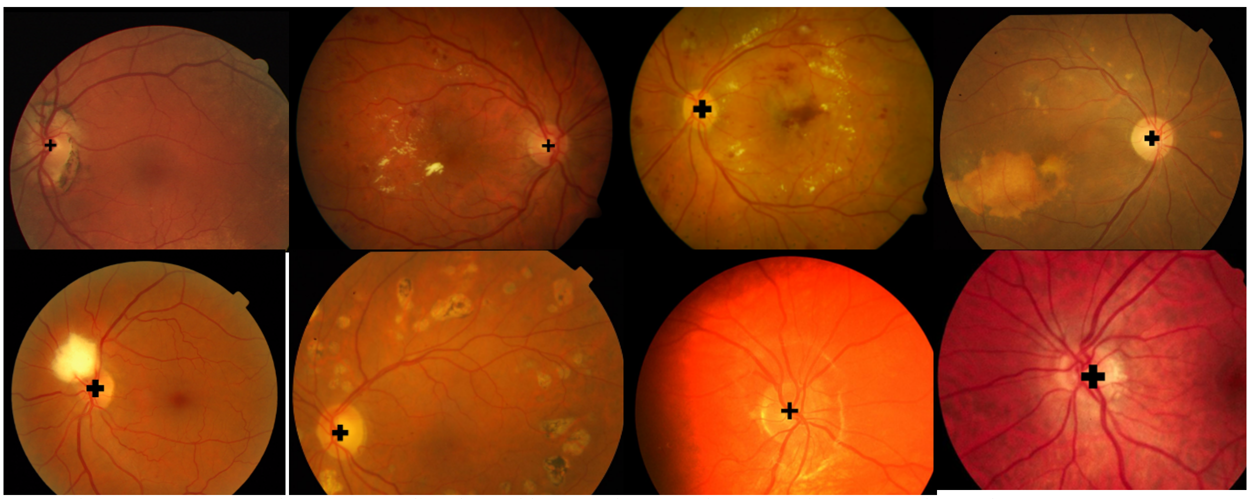

Figure 5 OD detection results. Sorting of images in rows is according to the following order DRIVE, DIARETDB1, Messidore, Shifa, CHASE_DB1 and DRIONS-DB

The OD detection method can correctly detect the OD center even in the presence of exudates and other pathologies. Accurate detection of the optic nerve head facilitates the segmentation algorithm to extract the boundary with high precision. OD segmentation results in Figure 6 clearly depict the ability of proposed method to segment, even with illumination artifacts when the OD boundary is not clear and in the presence of pathologies like papillary atrophy, which may increase the chances of false positives. The results of Grow Cut segmentation is further improved by an approximation process which can approximate both circular and elliptical shapes of the Grow Cut boundary.

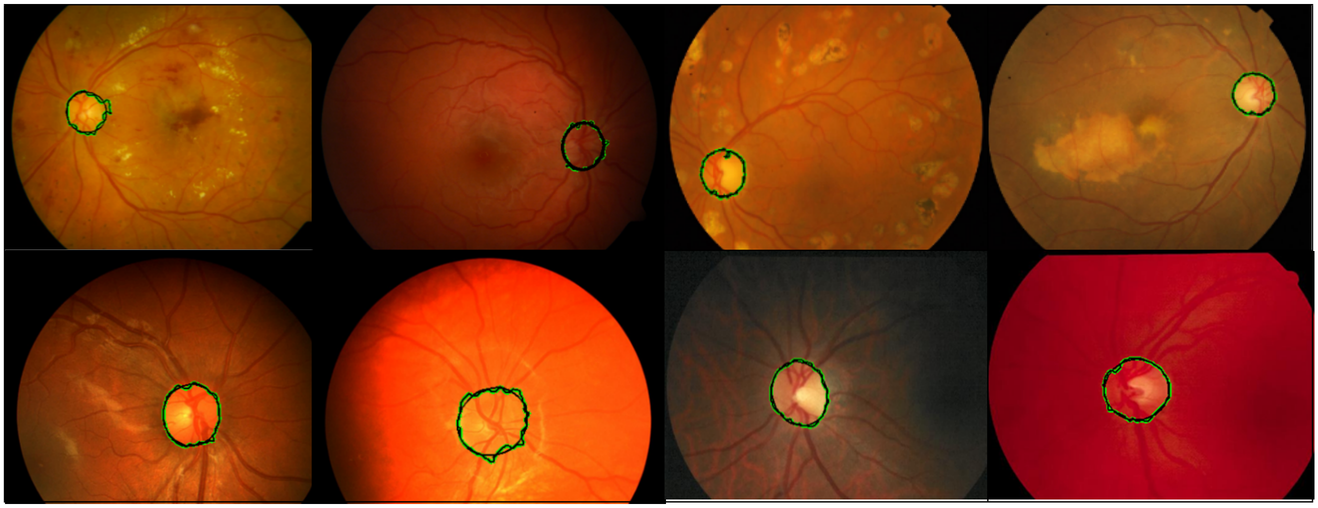

Figure 6 Examples of segmentation. Images in each row belong to separate databases as per order, DIARETDB1, Shifa, CHASE_DB1, and DRIONS-DB. Grow Cut segmentation is represented by a green boundary and its final approximation is represented by a black circle.

5 Discussion and Conclusion

Optic disc segmentation is the primary step towards the development of automatic screening systems. The accuracy of the segmentation method improves the correct identification of pathological diseases like glaucoma. Similarly, optic disc detection is the first step towards segmentation and accurate detection would lead to promising segmentation results.

This paper presents a new method for automatic detection and segmentation of the OD in retinal images. Using morphological operations, Circular Hough Transform and Grow Cut algorithm (Vezhnevets & Konouchine 2005). The GC algorithm has been widely used in many application areas of image segmentation, but has not been applied within the framework of retinal image analysis. To the limit of our knowledge, the GC algorithm has been utilized for the first time in localizing and segmenting OD in retinal images. The method is evaluated on five retinal image datasets exhibiting different morphological characteristics. Experimental evaluation shows that this method is computationally fast in processing, robust to the variation in image contrast and illumination, and comparable with state-of-the-art methodologies in terms of quantitative performance metrics.

The work is aimed at contributing to the development of an automatic system for glaucoma detection that is currently under development. Although other published solutions can be used, this work presents higher accuracy, robustness and is tolerant to a vast variety of images which make it suitable for integration with a glaucoma detection system.

The methodology offers 100% OD detection rate in DRIVE, DIARETDB1, CHASE_DB1, and Shifa databases, and 99.09% success rate in DRIONS-DB1. For the OD segmentation we use the detected OD center point as the seed for the Grow Cut algorithm, which then iteratively searches for neighbors of initial seeds and expands the region based on the label and strength of each pixel. The proposed method is able to segment the OD with a better overlap ratio, as compared to other methods available in the literature. We achieved 78.6%, 85.1%, 83.2%, 80.1%, 85.1% and 87.93% in DRIVE, DIARETDB1, CHASE_DB1, Shifa, DRIONS-DB1 and Messidor databases respectively. The results of the presented algorithm can be seen online at http://vision.seecs.edu.pk/od/.

We have already developed a fully automated software system named QUARTZ (Fraz et al. 2015), which can extract a number of quantifiable measures from retinal vessel morphology. These measures are analyzed/studied by epidemiologists and other medical/statistical experts in order to evaluate the association of retinal vessel abnormalities with other systemic diseases. In future, we aim to enhance the aforementioned software system and extend its functionality by incorporating a module for early detection of glaucoma in large population based screening programs. The proposed method for reliable segmentation of OD can be seen as a first step towards the development of a glaucoma detection module.

Acknowledgment

The Authors would like to thank teams of DRIVE, DIARETDB1, CHASE_DB1, DRIONS-DB and Messidor for maintaining and keeping these databases active and making them easily accessible for researchers to carry out retinal image analysis research. Furthermore, we would also thank the experts from the Armed Forces Institute of Ophthalmology, Rawalpindi, Pakistan for taking the time to establish the ground truth images.

References

2004. DRIVE: Digital Retinal Images for Vessel Extraction.

Abramoff MD, Garvin MK, and Sonka M. 2010. Retinal Imaging and Image Analysis. *Biomedical Engineering, IEEE Reviews in* 3:169-208. 10.1109/rbme.2010.2084567

Aquino A, Gegúndez-Arias ME, and Marín D. 2010. Detecting the optic disc boundary in digital fundus images using morphological, edge detection, and feature extraction techniques. *Medical Imaging, IEEE Transactions on* 29:1860-1869.

Basit A, and Fraz MM. 2015. Optic disc detection and boundary extraction in retinal images. *Applied Optics* 54:3440-3447. 10.1364/ao.54.003440

Carmona EJ, Rincón M, García-Feijoó J, and Martínez-de-la-Casa JM. 2008. Identification of the optic nerve head with genetic algorithms. *Artificial Intelligence in Medicine* 43:243-259.

Cheng J, Liu J, Xu Y, Yin F, Wong DWK, Tan N-M, Tao D, Cheng C-Y, Aung T, and Wong TY. 2013. Superpixel classification based optic disc and optic cup segmentation for glaucoma screening. *Medical Imaging, IEEE Transactions on* 32:1019-1032.

Dashtbozorg B, Mendonça AM, and Campilho A. 2015. Optic disc segmentation using the sliding band filter. *Computers in biology and medicine* 56:1-12.

Decenciere E, Zhang X, Cazuguel G, Laÿ B, Cochener B, Trone C, Gain P, Ordónez-Varela J-R, Massin P, and Erginay A. 2014. Feedback on a publicly distributed image database: the MESSIDOR database. *Image Analysis and Stereology*:231-234.

Federation ID. 2013. International Diabetic Federation Atlas; Chapter 2 The Gobal Burden. *Available at http://www.idf.org/sites/default/files/EN_6E_Ch2_the_Global_Burden.pdf* (accessed 3 December 2015).

Foracchia M, Grisan E, and Ruggeri A. 2005. Luminosity and contrast normalization in retinal images. *Medical image analysis* 9:179-190. 10.1016/j.media.2004.07.001

Fraz MM, Basit A, and Barman SA. 2012a. Application of Morphological Bit Planes in Retinal Blood Vessel Extraction. *Journal of Digital Imaging*:1-13. 10.1007/s10278-012-9513-3

Fraz MM, Remagnino P, Hoppe A, Uyyanonvara B, Rudnicka AR, Owen CG, and Barman SA. 2012b. Blood vessel segmentation methodologies in retinal images – A survey. *Computer methods and programs in biomedicine* 108:407-433.

Fraz MM, Remagnino P, Hoppe A, Uyyanonvara B, Rudnicka AR, Owen CG, and Barman SA. 2012c. An Ensemble Classification-Based Approach Applied to Retinal Blood Vessel Segmentation. *Biomedical Engineering, IEEE Transactions on* 59:2538-2548. 10.1109/TBME.2012.2205687

Fraz MM, Rudnicka A, Owen C, and Barman S. 2014. Delineation of blood vessels in pediatric retinal images using decision trees-based ensemble classification. *International Journal of Computer Assisted Radiology and Surgery* 9:795-811. 10.1007/s11548-013-0965-9

Fraz MM, Welikala RA, Rudnicka AR, Owen CG, Strachan DP, and Barman SA. 2015. QUARTZ: Quantitative Analysis of Retinal Vessel Topology and size – An automated system for quantification of retinal vessels morphology. *Expert Systems with Applications* 42:7221-7234. http://dx.doi.org/10.1016/j.eswa.2015.05.022

Haleem MS, Han L, van Hemert J, and Li B. 2013. Automatic extraction of retinal features from colour retinal images for glaucoma diagnosis: A review. *Computerized Medical Imaging and Graphics* 37:581-596.

Hoover A, and Goldbaum M. 2003. Locating the optic nerve in a retinal image using the fuzzy convergence of the blood vessels. *Medical Imaging, IEEE Transactions on* 22:951-958.

Hough PV. 1962. Method and means for recognizing complex patterns.

Hsiao H-K, Liu C-C, Yu C-Y, Kuo S-W, and Yu S-S. 2012. A novel optic disc detection scheme on retinal images. *Expert Systems with Applications* 39:10600-10606.

Illingworth J, and Kittler J. 1987. The Adaptive Hough Transform. *Pattern Analysis and Machine Intelligence, IEEE Transactions on* PAMI-9:690-698. 10.1109/tpami.1987.4767964

Jack J. Kanski, and Brad Bowling. 2015. *Clinical Ophthalmology: A Systematic Approach*. London: Elsevier Health Sciences (UK).

Joshi GD, Sivaswamy J, and Krishnadas S. 2011. Optic disk and cup segmentation from monocular color retinal images for glaucoma assessment. *Medical Imaging, IEEE Transactions on* 30:1192-1205.

Kande GB, Subbaiah PV, and Savithri TS. 2008. Segmentation of exudates and optic disk in retinal images. Computer Vision, Graphics & Image Processing, 2008 ICVGIP'08 Sixth Indian Conference on: IEEE. p 535-542.

Kauppi T, Kalesnykiene V, Kamarainen J-K, Lensu L, Sorri I, Raninen A, Voutilainen R, Pietilä J, Kälviäinen H, and Uusitalo H. 2007. DIARETDB1 diabetic retinopathy database and evaluation protocol. Medical Image Understanding and Analysis (MIUA2007). Aberystwyth, Wales, UK. p 61-65.

Lu S. 2011. Accurate and efficient optic disc detection and segmentation by a circular transformation. *Medical Imaging, IEEE Transactions on* 30:2126-2133.

Lupascu CA, Tegolo D, and Rosa LD. 2008. Automated detection of optic disc location in retinal images. Computer-Based Medical Systems, 2008 CBMS'08 21st IEEE International Symposium on: IEEE. p 17-22.

Marin D, Gegundez-Arias ME, Suero A, and Bravo JM. 2015. Obtaining optic disc center and pixel region by automatic thresholding methods on morphologically processed fundus images. *Computer methods and programs in biomedicine* 118:173-185.

Mendonca AM, Sousa A, Mendonca L, and Campilho A. 2013. Automatic localization of the optic disc by combining vascular and intensity information. *Computerized Medical Imaging and Graphics* 37:409-417.

Mittapalli PS, and Kande GB. 2016. Segmentation of optic disk and optic cup from digital fundus images for the assessment of glaucoma. *Biomedical Signal Processing and Control* 24:34-46.

Morales S, Naranjo V, Angulo J, and Alcañiz M. 2013. Automatic detection of optic disc based on PCA and mathematical morphology. *Medical Imaging, IEEE Transactions on* 32:786-796.

Niemeijer M, Abràmoff MD, and Van Ginneken B. 2009. Fast detection of the optic disc and fovea in color fundus photographs. *Medical image analysis* 13:859-870.

Pourreza-Shahri R, Tavakoli M, and Kehtarnavaz N. 2014. Computationally efficient optic nerve head detection in retinal fundus images. *Biomedical Signal Processing and Control* 11:63-73.

Salazar-Gonzalez A, Kaba D, Li Y, and Liu X. 2014. Segmentation of the Blood Vessels and Optic Disk in Retinal Images. *Biomedical and Health Informatics, IEEE Journal of* 18:1874-1886.

Seo J, Kim K, Kim J, Park K, and Chung H. 2004. Measurement of ocular torsion using digital fundus image. Engineering in Medicine and Biology Society, 2004 IEMBS'04 26th Annual International Conference of the IEEE: IEEE. p 1711-1713.

Sopharak A, Uyyanonvara B, Barman S, and Williamson TH. 2008. Automatic detection of diabetic retinopathy exudates from non-dilated retinal images using mathematical morphology methods. *Computerized Medical Imaging and Graphics* 32:720-727. http://dx.doi.org/10.1016/j.compmedimag.2008.08.009

Stapor K, Świtonski A, Chrastek R, and Michelson G. 2004. Segmentation of fundus eye images using methods of mathematical morphology for glaucoma diagnosis. *Computational Science-ICCS 2004*: Springer, 41-48.

Toffoli T, and Margolus N. 1987. *Cellular automata machines: a new environment for modeling*: MIT Press.

Vázquez SG, Cancela B, Barreira N, Penedo MG, Rodríguez-Blanco M, Pena Seijo M, Tuero GC, Barceló MA, and Saez M. 2013. Improving retinal artery and vein classification by means of a minimal path approach. *Machine Vision and Applications* 24:919-930. 10.1007/s00138-012-0442-4

Vezhnevets V, and Konouchine V. 2005. GrowCut: Interactive multi-label ND image segmentation by cellular automata. proc of Graphicon: Citeseer. p 150-156.

Walter T, Klein J-C, Massin P, and Erginay A. 2002. A contribution of image processing to the diagnosis of diabetic retinopathy-detection of exudates in color fundus images of the human retina. *Medical Imaging, IEEE Transactions on* 21:1236-1243.

Weinreb RN, Aung T, and Medeiros FA. 2014. The pathophysiology and treatment of glaucoma: A review. *JAMA* 311:1901-1911. 10.1001/jama.2014.3192

Welfer D, Scharcanski J, Kitamura CM, Dal Pizzol MM, Ludwig LW, and Marinho DR. 2010. Segmentation of the optic disk in color eye fundus images using an adaptive morphological approach. *Computers in biology and medicine* 40:124-137.

Welfer D, Scharcanski J, and Marinho DR. 2013. A morphologic two-stage approach for automated optic disk detection in color eye fundus images. *Pattern Recognition Letters* 34:476-485.

Youssif AA-HA-R, Ghalwash AZ, and Ghoneim AASA-R. 2008. Optic disc detection from normalized digital fundus images by means of a vessels' direction matched filter. *Medical Imaging, IEEE Transactions on* 27:11-18.